Downloaded from orbit.dtu.dk on: Aug 21, 2018

Technical University of Denmark

On the truncation of the azimuthal mode spectrum of high-order probes in probe-corrected spherical near-field antenna measurements

Pivnenko, Sergey; Laitinen, Tommi

Published in:
Proceedings of the 33rd Annual Symposium of the Antenna Measurement Techniques Association

Publication date:
2011

Link back to DTU Orbit

Citation (APA):
Pivnenko, S., & Laitinen, T. (2011). On the truncation of the azimuthal mode spectrum of high-order probes in probe-corrected spherical near-field antenna measurements. In Proceedings of the 33rd Annual Symposium of the Antenna Measurement Techniques Association

DTU Library
Technical Information Center of Denmark

General rights
Copyright and moral rights for the publications made accessible in the public portal are retained by the authors and/or other copyright owners and it is a condition of accessing publications that users recognise and abide by the legal requirements associated with these rights.

- Users may download and print one copy of any publication from the public portal for the purpose of private study or research.
- You may not further distribute the material or use it for any profit-making activity or commercial gain
- You may freely distribute the URL identifying the publication in the public portal

If you believe that this document breaches copyright please contact us providing details, and we will remove access to the work immediately and investigate your claim.

ON THE TRUNCATION OF THE AZIMUTHAL MODE SPECTRUM OF HIGH-ORDER PROBES IN PROBE-CORRECTED SPHERICAL NEAR-FIELD ANTENNA MEASUREMENTS

Tommi Laitinen
Aalto University School of Electrical Engineering, Department of Radio Science and Engineering
P. O. Box 13000, 00076 AALTO, Finland

Sergey Pivnenko
Department of Electrical Engineering, Technical University of Denmark
2800 Kgs. Lyngby, Denmark

ABSTRACT

Azimuthal mode (μ mode) truncation of a high-order probe pattern in probe-corrected spherical near-field antenna measurements is studied in this paper. The results of this paper provide rules for appropriate and sufficient μ-mode truncation for non-ideal first-order probes and odd-order probes with approximately 10dBi directivity. The presented azimuthal mode truncation rules allow minimizing the measurement burden of the probe pattern calibration and reducing the computational burden of the probe pattern correction.

Keywords: Near-field measurement, probe correction.

1.0 Introduction

Probe-corrected spherical near-field measurements are an accurate technique for antenna pattern characterization [1]. In such measurements, truncated form of the spherical wave expansion is typically used for pattern modeling of both the antenna under test and the probe. It is often assumed that the probe is a so-called first-order (μ = ±1) probe [2] and, in modeling of the probe pattern, only the first-order azimuthal pattern variations are present, while the other azimuthal modes are assumed zero.

Recently, higher-order probe correction techniques have gained a lot of interest among the antenna measurement research community [3]-[7]. In the application of such techniques, in addition to the azimuthal modes with μ = ±1, also the azimuthal modes with $\mu \neq \pm 1$ are included in the modeling of the probe pattern. This facilitates the use of very wideband antennas as probes [8].

The purpose of this paper is to study how the truncation of the azimuthal modes of the probe is to be performed in probe-corrected spherical near-field antenna measurements with high-order probes. The results of this paper provide rules for appropriate and sufficient μ-mode truncation for a probe with approximately 10dBi directivity. The study is based on computer simulations, and two classes of probe are taken for a detailed investigation. The first class of probes represents non-ideal first-order probes whereas the other class of probes represents odd-order probes. The presented μ-mode truncation rules allow minimizing the measurement burden of the probe pattern calibration and reducing the computational burden of the probe pattern correction.

This paper is organized as follows. Section 2.0 describes the background theory. Computer calculations are presented in Section 3.0. Section 4.0 is devoted to results and Section 5.0 presents the conclusions.

2.0 Background theory

The background theory for the study of this paper is based on the theory of the probe-corrected spherical near-field antenna measurements presented in [2]. According to this theory, the AUT and the probe patterns are described by means of spherical wave expansion (SWE). Through the use of the spherical wave rotations and translations, the so-called transmission formula is established that provides an analytical formula for the received signal of the probe as a function of the unknown spherical vector wave coefficients (Q coefficients) of the AUT pattern. The solving of the transmission formula for the Q coefficients and calculation of the far field from the SWE of the AUT pattern constitutes essentially the probe-corrected near-field to far-field transformation.

The SWE of the probe is expressed as

$$\overline{E}(r',\theta',\phi') = \frac{k}{\sqrt{\eta}} \sum_{\sigma=1}^{2} \sum_{\nu=1}^{\nu_{\max}} \sum_{\substack{\mu=-\mu_{\max} \\ (|\mu|\leq\nu)}}^{\mu_{\max}} (-1)^{\mu} R_{\sigma-\mu\nu} \overline{F}^{(3)}_{\sigma\mu\nu}(r',\theta',\phi') \tag{1}$$

where (r',θ',ϕ') are the standard spherical coordinates of the probe coordinate system, k is the wave number, η is the intrinsic admittance of the medium, ν_{max} and μ_{max} are the truncation numbers for the spherical wave expansion, $R_{\sigma\mu\nu}$ are the probe receiving coefficients, and $\overline{F}^{(3)}_{smn}(r,\theta,\phi)$ are the spherical vector wave functions [2].

3.0 Calculations

Our interest is now to study by computer calculations the effects of the truncation of the μ-mode summation in Eq. (1) on the accuracy of the far-field determination in probe-corrected spherical near-field antenna measurements. The double ϕ-step θ-scanning technique and the associated high-order probe correction technique [3] and also the ϕ-scanning technique and the associated high-order probe correction technique [4] are included in the study. These calculations are described in this section.

3.1 AUT models

In total 4 different AUT models (AUT1 to AUT4) are applied in the calculations. Each AUT model consists of 4 x-oriented Huygens sources located on the corners of a $\lambda \times \lambda$ square on z plane. Each Huygens source has the same phase and maximum radiation in the +z-axis direction. The 4 AUT models differ from each other only in the location of the centre of the Huygens source square. For the AUT1 to AUT4, the (x, y, z) coordinates of the centre of the Huygens source square are (0, 0, 0)λ, (1, 0, 0)λ, (2, 0, 0)λ, and (3, 0, 0)λ, respectively. In other words, the AUT1 is centred in the AUT coordinate system, and in the case of the AUT2 to AUT4, the Huygens source square is located at an offset distance along +x axis from the centre of the AUT coordinate system. The patterns of AUT1 to AUT4 are the same expect for the phase. The co-polar directivity of the AUT1 is presented in Fig. 1.

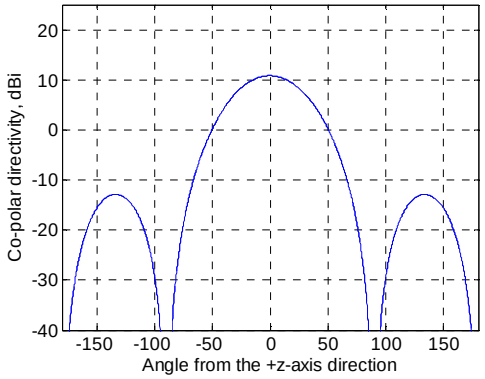

Figure 1 - The co-polar directivity of AUT1 for $\phi = 0°$ plane. The co-polar directivity is the same for the $\phi = 90°$ plane.

3.2 Probe models

The starting point for creating high-order probes for this study was the creation of a first-order probe consisting of 9 x-oriented electric Hertzian dipoles located with $\lambda/4$ intervals on z axis from $z = -\lambda$ to λ range. The excitations of the dipoles 1 to 9 are $\exp(-jp\pi/2)$ where $p = -4 \ldots 4$ for dipole 1…9, respectively. The main beam of the probe is pointed towards $-z$ axis, that is, towards the centre of the AUT coordinate system in the computer calculations. The pattern of this probe with the main beam pointed towards +z-axis direction is shown in Fig. 2. The maximum co-polar directivity of this first-order probe is 10 dBi.

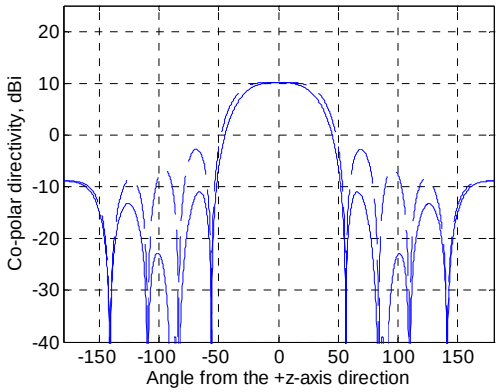

Figure 2 - The pattern of the first-order probe consisting of 9 x-oriented electric Hertzian dipoles located with $\lambda/4$ intervals on z axis from $z = -\lambda$ to λ range.

Next, for the purposes of this study, two different classes of high-order probes are created by exploiting the first-order probe consisting of 9 electric Hertzian dipoles.

For the first class of high-order probes, first the receiving coefficients ($R_{1-1\nu}, R_{11\nu}, R_{2-1\nu}, R_{21\nu}$ for $\nu = 1 \ldots \nu_{\max}$) of this first-order probe are calculated. Then, for each fixed ν, the receiving coefficients with $R_{10\nu}$ are $R_{20\nu}$ are given random values $\alpha\exp(j\beta 2\pi)$, where α is a real-valued amplitude, and β is a random number between 0 and 1, such that the power in mode with $R_{10\nu}$ is the same as the power in mode with $R_{20\nu}$ (that is, α is the same for these two, but the β is generally different) and the total power in modes with $R_{10\nu}$ and $R_{20\nu}$ is X dB below the power in modes with $R_{1-1\nu}$, $R_{2-1\nu}$, $R_{11\nu}$ and $R_{21\nu}$. Further, for each fixed ν (for $\nu > 1$) and for each fixed $\mu = 2 \ldots \nu$ the receiving coefficients with $R_{1-\mu\nu}$, $R_{2-\mu\nu}$, $R_{1\mu\nu}$, and $R_{2\mu\nu}$ are similarly given random values $\alpha\exp(j\beta 2\pi)$ such that the power in all modes $R_{1-\mu\nu}$, $R_{2-\mu\nu}$, $R_{1\mu\nu}$, and $R_{2\mu\nu}$ is the same, and the total power in modes with $R_{1-\mu\nu}$, $R_{2-\mu\nu}$, $R_{1\mu\nu}$, and $R_{2\mu\nu}$ is X dB below the power in modes with $R_{1-1\nu}$, $R_{2-1\nu}$, $R_{11\nu}$ and $R_{21\nu}$. The X is chosen in this study to be −20 dB or −30 dB. In this paper, the 2 different cases are referred to as the probe with X = −20 dB and −30 dB. In this way, power spectra shown in Figs. 3(a)-(b) are obtained for the probes with X = −20 dB and −30 dB.

The second class of probes comprises in total 27 electric Hertzian dipoles. Nine of these 27 dipoles are the same as those of the above-described first-probes with the amplitude of each of the excitation coefficients equalling to 1. The remaining 18 dipoles are located similarly (in sets of 9 dipoles) with $\lambda/4$ intervals in the $z = -\lambda$ to λ

range. The first set of 9 dipoles is located on the y-z plane (x = 0) at the distance of 1 λ towards +y-axis direction parallel to the z axis, and the other set of 9 dipoles is located on the y-z plane (x = 0) at the distance of 1 λ towards $-y$-axis direction parallel to the z-axis. The excitations for the two sets of 9 dipoles, that are not located on z axis, are γ times the excitations of the corresponding dipoles located on z axis. The γ is given values of 1, 0.3 and 0.1 in order to create odd-order probes with varying spherical azimuthal mode power in modes with μ = 3, 5, 7 etc. Later in this paper, these different cases are referred to as probes with γ = 1, 0.3 and 0.1. The normalised spherical μ-mode power spectra for these probes are shown in Figs. 4(a)-(c).

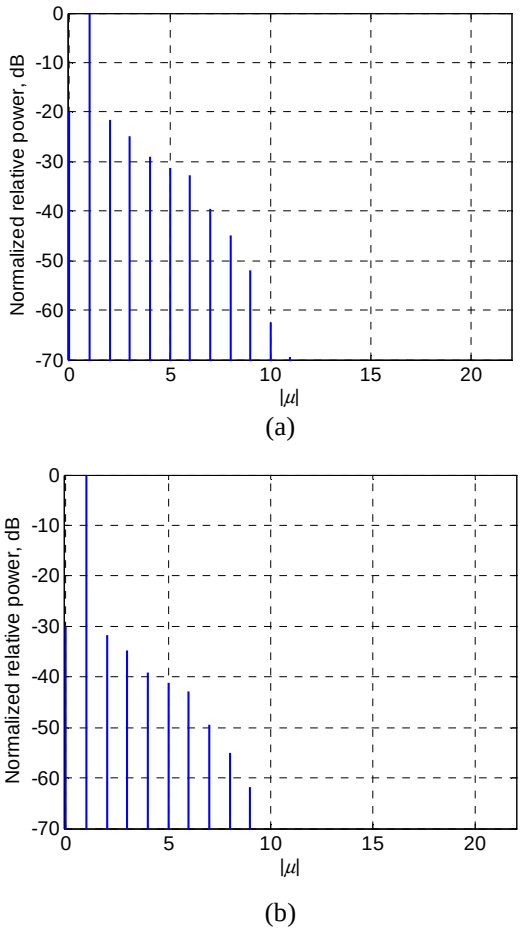

(a)

(b)

Figure 3 - The normalised spherical μ-mode power spectra for the probes with X = –20 dB (a) and X = –30 dB (b).

3.3 Computer calculations

First, for each probe model, the probe received signals are calculated from the transmission formula for the measurement distance r = 6λ for each AUT model. The truncation numbers for the AUT1 to AUT4 are N = M = 12, 18, 24, and 30, respectively. Here N and M are the truncation numbers of the SWE of the AUT pattern and correspond to those of ν_{max} and μ_{max} of the SWE of the probe pattern [2]. Then, in the application of the probe correction technique based on the double ϕ-step θ-scanning, the probe signals for two polarizations of the probe are calculated for those θ and ϕ angles that correspond to the sampling parameter values of N_θ' = 2(N + 1) and N_ϕ' = M + 3 of the double ϕ-step θ-scanning technique [3]. In the case of the probe correction technique based on the ϕ-scanning the probe signals are calculated for those θ and ϕ angles that correspond to the values of N_θ = N + 2 and N_ϕ = 2M + 6. Next, the probe correction technique associated with the double ϕ-step θ-scanning scheme and that associated with the ϕ-scanning scheme are applied on the received signals to calculate the estimated Q coefficients of each AUT models for varying μ-mode truncation numbers for μ_{max} = 1 to 7. The radiated far field associated with each set of these Q coefficients is then calculated. In this way, in total 2×181×360 = 130320 estimated far-field values are obtained for each examined case. Here, the number 2 refers to two polarizations of the far field, the number 181 refers to the number of θ angles and the number 360 refers to the number of ϕ angles.

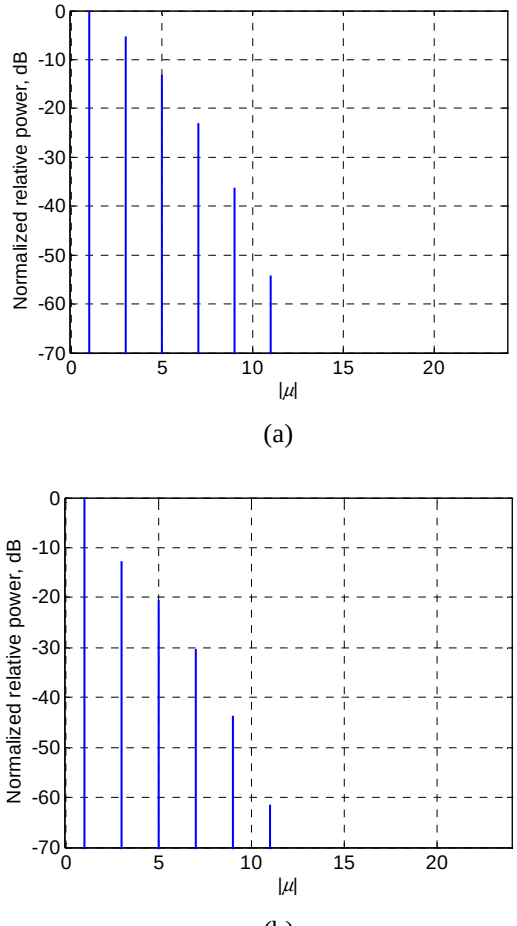

(a)

(b)

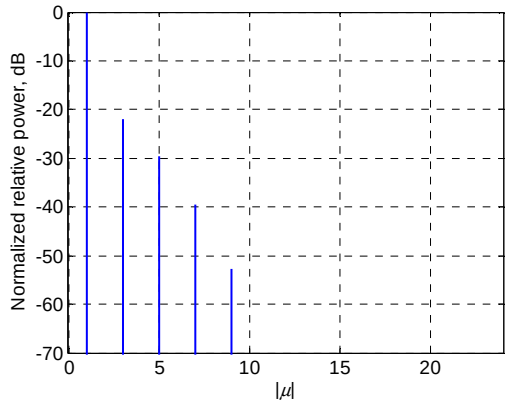

(c)

Figure 4 - The normalised spherical μ-mode power spectra for the probe with γ= 1 (a), γ= 0.3 (d) and γ= 0.1 (e).

4.0 Results

Example results from the calculations are presented in Fig. 5 for AUT2 with the high-order probe with X = –30 dB for μ_{max} = 1, where the amplitude errors ε in terms of $|20\log10(E_p)–20\log10(E_c)|$, where E_p and E_c are the estimated (with a certain μ_{max}) and correct far-field values, respectively, are plotted as a function of q, where q is the level of the far-field value compared to the maximum far-field value. It can be stated from the results that for the first class of probes, generally, the double ϕ-step θ-scanning scheme provides slightly more accurate estimate of the far field than the ϕ-scanning scheme for a fixed value of μ_{max}. For the second class of probes both schemes provide the same results.

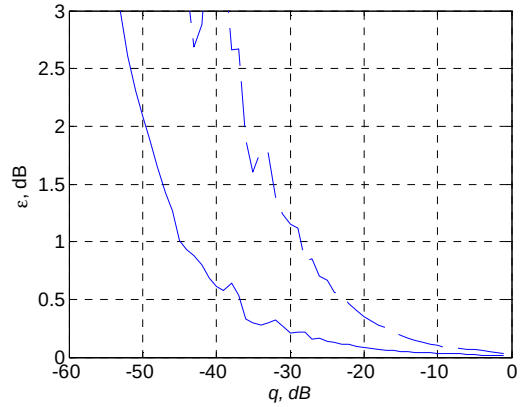

Figure 5 - The amplitude [ε, dB] errors for double ϕ-step θ-scanning scheme (solid line) and for ϕ-scanning scheme (dashed line) for AUT2 with the high-order probe with X = –30 dB for μ_{max} = 1 as a function of the level of the far-field value compared to the maximum far-field value

In Tables 1-5, the required truncation numbers for reaching an amplitude uncertainty of e_{max} (in terms of ε in dB) or lower and phase uncertainty of d_{max} or lower are presented for different ratios r/r_0 for a given q range for all probe and AUT models for the case with double ϕ-step θ-scanning scheme. The d_{max} is determined in terms of $|\text{Ang}(E_p)–\text{Ang}(E_c)|$ values, where "Ang" gives the phase angle of a far-field component. The r/r_0 refers to the ratio between the measurement distance and the radius of the AUT minimum sphere. Hence, the cases with $r/r_0 \approx$ 8.5, 3.8, 2.4 and 1.7 refer to AUT1 to AUT4, respectively.

The results for the first class of probes are presented in Tables 1 and 2. In summary, it can be stated from the results that for the case of the probe with the relative power of X = –30 dB of the higher-order modes, the correction for the μ-modes up to μ_{max} = 1 was sufficient for reaching the maximum error of less than 0.1 dB in the co-polar directivity in the q range of 0 to –10 dB for $r/r_0 \approx$ 3.8 or higher. The values of μ_{max} = 2 and 4 were required for $r/r_0 \approx$ 2.4 and 1.7, respectively. The same values of μ_{max} were actually required also for reaching the maximum phase error of 0.5° or less. The errors gradually increase with increasing level of power in modes with $|\mu| \neq 1$ with respect to the power in modes with $|\mu| = 1$.

The results for the second class of high-order probes are presented in Tables 3 to 5. The results, for example, for the probe with the relative power in the third, fifth and seventh order μ modes of the order of –5 dB, –12 dB, and –22 dB (γ = 1.0 case) show that μ_{max} = 2 is sufficient for reaching the maximum error of less than 0.1 dB in the co-polar directivity in the q range of 0 to –10 dB for $r/r_0 \approx$ 3.8 or higher, and μ_{max} = 7 is required for $r/r_0 \approx$ 2.4 and $r/r_0 \approx$ 1.7. The results for the phase follow the same trend. With decreasing power in the higher order modes, the required truncation numbers gradually decrease.

5.0 Summary and conclusions

The effects of the azimuthal spherical mode truncation of the probe pattern on the accuracy of the far-field determination with non-ideal first-order probes and odd-order probes with a 10-dBi directivity have been studied. The results of this paper provide azimuthal mode truncation rules that allow minimizing the measurement burden of the probe pattern calibration and reducing the computational burden of the probe pattern correction.

6. REFERENCES

[1] A. Yaghjian, "An overview of near-field antenna measurements," *IEEE Transactions on Antennas and Propagation*, Vol. 34, No. 1, Jan. 1986, pp. 30-45.

[2] J. E. Hansen (ed.), *Spherical Near-Field Antenna Measurements*, Peter Peregrinus, Ltd., London, 1988.

[3] T. A. Laitinen, "Double ϕ-step θ-scanning technique for spherical near-field antenna measurements," *IEEE Transactions on Antennas and Propagation*, vol. 56, no. 6, pp. 1633-1639, June 2008.

[4] T. A. Laitinen, S. Pivnenko, J. Mailund Nielsen, and O. Breinbjerg, "Theory and practice of the FFT/matrix inversion technique for probe-corrected spherical near-field antenna measurements with high-order probes," *IEEE Transactions on Antennas and Propagation*, vol. 58, no. 8, pp. 2623-2631, Aug. 2010.

[5] C. Schmidt and T. Eibert, "Multi plane wave based near-field far-field transformation for electrically large antennas in free-space or above material halfspace," *IEEE Transactions on Antennas and Propagation*, vol. 57, no. 5, pp. 1382-1390, May 2009.

[6] T. B. Hansen, "Complex-point dipole formulation of probe-corrected cylindrical and spherical near-field scanning of electromagnetic fields," *IEEE Transactions on Antennas and Propagation*, vol. 57, no. 3, pp. 728-741, March 2009.

[7] T. Laitinen, S. Pivnenko, and O. Breinbjerg, "Iterative probe correction technique for spherical near-field antenna measurements," *IEEE Antennas and Wireless Propagation Letters*, vol. 4, pp. 221-223, 2005.

[8] T. Laitinen, S. Pivnenko, J.M. Nielsen, and O. Breinbjerg, *Development of 1-3GHz Probes for the DTU-ESA Spherical Near-Field Antenna Test Facility, ESTEC Contract No. 18222/04/NL/LvH/bj, Final Report, Vol. 1: Executive Summary*, Technical University of Denmark, R729, Dec. 2006.

7. ACKNOWLEDGMENTS

The authors of this paper would like to thank European Space Agency for the financial support of this work carried out under the ESA contract No. 22812/09/NL/JD/al. T. Laitinen would like to thank also Academy of Finland for the financial support of the work.

Table 1: The required truncation number for a probe with X = –20 dB.

	Amplitude					Phase				
q range [dB]	$e_{max,}$ [dB]	$r/r_0 \approx 8.5$	$r/r_0 \approx 3.8$	$r/r_0 \approx 2.4$	$r/r_0 \approx 1.7$	$d_{max,}$ [deg.]	$r/r_0 \approx 8.5$	$r/r_0 \approx 3.8$	$r/r_0 \approx 2.4$	$r/r_0 \approx 1.7$
0 … –10	0.1	1	1	2	4	0.5	1	1	3	4
	0.2	1	1	2	4	1.0	1	1	3	4
	0.5	1	1	1	4	3.0	1	1	1	4
	1.0	1	1	1	3	5.0	1	1	1	4
0 … –20	0.1	1	3	3	6	0.5	1	3	4	6
	0.2	1	3	3	5	1.0	1	3	3	6
	0.5	1	1	2	4	3.0	1	1	2	4
	1.0	1	1	2	4	5.0	1	1	2	4
0 … –30	0.1	2	3	5	7	0.5	2	3	5	7
	0.2	1	3	4	6	1.0	1	3	5	7
	0.5	1	3	3	6	3.0	1	3	3	5
	1.0	1	1	2	4	5.0	1	1	3	4
0 … –40	0.1	2	3	5	7	0.5	2	4	5	7
	0.2	2	3	5	7	1.0	2	3	5	7
	0.5	1	3	5	6	3.0	1	3	5	7
	1.0	1	3	3	6	5.0	1	3	3	6

Table 2: The required truncation number for a probe with X = –30 dB.

	Amplitude					Phase				
q range [dB]	$e_{max,}$ [dB]	$r/r_0 \approx 8.5$	$r/r_0 \approx 3.8$	$r/r_0 \approx 2.4$	$r/r_0 \approx 1.7$	$d_{max,}$ [deg.]	$r/r_0 \approx 8.5$	$r/r_0 \approx 3.8$	$r/r_0 \approx 2.4$	$r/r_0 \approx 1.7$
0 … –10	0.1	1	1	2	4	0.5	1	1	2	4
	0.2	1	1	1	4	1.0	1	1	1	4
	0.5	1	1	1	2	3.0	1	1	1	2
	1.0	1	1	1	1	5.0	1	1	1	1
0 … –20	0.1	1	1	3	5	0.5	1	2	3	5
	0.2	1	1	3	5	1.0	1	1	2	4
	0.5	1	1	2	4	3.0	1	1	2	4
	1.0	1	1	1	2	5.0	1	1	1	3
0 … –30	0.1	1	3	4	6	0.5	1	3	4	7
	0.2	1	2	3	5	1.0	1	3	3	6
	0.5	1	1	3	5	3.0	1	1	2	4
	1.0	1	1	2	4	5.0	1	1	2	4
0 … –40	0.1	1	3	4	7	0.5	2	3	4	7
	0.2	1	3	4	7	1.0	1	3	4	7
	0.5	1	2	3	5	3.0	1	3	3	6
	1.0	1	1	3	5	5.0	1	2	3	5

Table 3: The required truncation numbers for a probe with $\gamma = 1.0$.

	Amplitude					Phase				
q range [dB]	$e_{max,}$ [dB]	$r/r_0 \approx 8.5$	$r/r_0 \approx 3.8$	$r/r_0 \approx 2.4$	$r/r_0 \approx 1.7$	$d_{max,}$ [deg.]	$r/r_0 \approx 8.5$	$r/r_0 \approx 3.8$	$r/r_0 \approx 2.4$	$r/r_0 \approx 1.7$
0 … –10	0.1	2	2	7	7	0.5	1	3	7	9
	0.2	1	2	5	7	1.0	1	2	5	7
	0.5	1	2	5	7	3.0	1	2	5	7
	1.0	1	2	5	5	5.0	1	2	5	5
0 … –20	0.1	2	3	7	9	0.5	2	3	7	9
	0.2	2	3	7	7	1.0	1	3	7	9
	0.5	1	2	5	7	3.0	1	2	5	7
	1.0	1	2	5	7	5.0	1	2	5	7
0 … –30	0.1	2	3	7	9	0.5	2	3	7	9
	0.2	2	3	7	9	1.0	2	3	7	9
	0.5	1	3	5	7	3.0	1	2	5	7
	1.0	1	2	5	7	5.0	1	2	5	7
0 … –40	0.1	2	3	7	9	0.5	2	3	7	9
	0.2	2	3	7	9	1.0	2	3	7	9
	0.5	2	3	7	9	3.0	1	3	7	9
	1.0	1	3	5	7	5.0	1	3	7	9

Table 4: The required truncation numbers for a probe with $\gamma = 0.3$.

	Amplitude					Phase				
q range [dB]	$e_{max,}$ [dB]	$r/r_0 \approx 8.5$	$r/r_0 \approx 3.8$	$r/r_0 \approx 2.4$	$r/r_0 \approx 1.7$	$d_{max,}$ [deg.]	$r/r_0 \approx 8.5$	$r/r_0 \approx 3.8$	$r/r_0 \approx 2.4$	$r/r_0 \approx 1.7$
0 … –10	0.1	1	2	5	7	0.5	1	2	5	7
	0.2	1	2	5	7	1.0	1	2	5	7
	0.5	1	2	5	5	3.0	1	2	5	5
	1.0	1	2	3	5	5.0	1	2	3	5
0 … –20	0.1	2	3	5	7	0.5	1	3	7	7
	0.2	1	2	5	7	1.0	1	2	5	7
	0.5	1	2	5	7	3.0	1	2	5	7
	1.0	1	2	5	7	5.0	1	2	5	7
0 … –30	0.1	2	3	7	9	0.5	2	3	7	9
	0.2	1	3	5	7	1.0	1	3	7	7
	0.5	1	2	5	7	3.0	1	2	5	7
	1.0	1	2	5	7	5.0	1	2	5	7
0 … –40	0.1	2	3	7	9	0.5	2	3	7	9
	0.2	2	3	7	9	1.0	1	3	7	9
	0.5	1	3	7	7	3.0	1	3	7	7
	1.0	1	3	5	7	5.0	1	2	5	7

Table 5: The required truncation numbers for a probe with $\gamma = 0.1$.

	Amplitude					Phase				
q range [dB]	$e_{max,}$ [dB]	$r/r_0 \approx 8.5$	$r/r_0 \approx 3.8$	$r/r_0 \approx 2.4$	$r/r_0 \approx 1.7$	$d_{max,}$ [deg.]	$r/r_0 \approx 8.5$	$r/r_0 \approx 3.8$	$r/r_0 \approx 2.4$	$r/r_0 \approx 1.7$
0 … –10	0.1	1	2	5	7	0.5	1	2	5	7
	0.2	1	2	5	5	1.0	1	2	5	5
	0.5	1	1	3	5	3.0	1	1	3	5
	1.0	1	1	3	5	5.0	1	1	3	5
0 … –20	0.1	1	2	5	7	0.5	1	2	5	7
	0.2	1	2	5	7	1.0	1	2	5	7
	0.5	1	2	5	5	3.0	1	2	3	7
	1.0	1	2	3	5	5.0	1	2	3	5
0 … –30	0.1	1	3	5	7	0.5	1	2	5	7
	0.2	1	2	5	7	1.0	1	2	5	7
	0.5	1	2	5	7	3.0	1	2	5	7
	1.0	1	2	5	7	5.0	1	2	5	7
0 … –40	0.1	2	3	7	9	0.5	1	3	7	9
	0.2	1	3	5	7	1.0	1	3	7	9
	0.5	1	2	5	7	3.0	1	2	5	7
	1.0	1	2	5	7	5.0	1	2	5	7